Jurnal Polimesin
Department of Mechanical Engineering
State Polytechnic of Lhokseumawe
http://e-jurnal.pnl.ac.id/polimesin
e-ISSN : 2549-1999 No. : 3 Month : June
p-ISSN : 1693-5462 Volume : 24 Year : 2026

Processing dates: received on 2026-3-23, reviewed on 2026-04-12, accepted on 2026-05-18 and online availability on 2026-06-30

Interfacial modification of high-loading sugar palm fiber/unsaturated polyester biocomposites using alkali–vinyltrimethoxysilane treatment

Fahriadi Pakaya*, Yurika Nantan, Marinus S. Tappy, I Nyoman Subawa
Fisheries Mechanization Study Program, Bitung Marine and Fisheries Polytechnic, Bitung 95525, Indonesia
*Corresponding author: fahriadi.pakaya@kkp.go.id

Abstract

Natural fiber-reinforced polyester biocomposites are promising lightweight materials, but their performance is often limited by weak fiber–matrix interaction, especially at high fiber loading. This study investigates the effect of combined alkali–Vinyltrimethoxysilane (VTMS) treatment on the flexural and physical properties of sugar palm fiber-reinforced Unsaturated Polyester Resin (UPR) biocomposites. Untreated fiber composites (IU/UPR), NaOH-treated fiber composites (IA/UPR), and NaOH–VTMS-treated fiber composites (IAS/UPR) were fabricated using the hand lay-up method at fiber loadings of 0–50 wt.%. The results showed that IAS/UPR exhibited the best overall performance, particularly at 50 wt.% fiber loading, achieving a flexural strength of 110.59 MPa, compared with 37.20 MPa for IU/UPR and 50.60 MPa for IA/UPR. IAS/UPR also showed lower water absorption, higher density, and lower porosity. Two-way ANOVA confirmed that fiber treatment, fiber loading, and their interaction significantly affected flexural strength, water absorption, and porosity. FTIR analysis indicated the reduction of hemicellulose and lignin-related components, while SEM observations showed improved matrix coverage, fewer interfacial gaps, and reduced fiber pull-out. These results indicate that alkali–VTMS treatment improves interfacial compatibility and extends the effective fiber-loading range of sugar palm fiber/UPR biocomposites.

Keywords:
Alkali treatment, flexural strength, physical properties, sugar palm fiber, unsaturated polyester resin.

1 Introduction

The use of natural fibers as reinforcements in polymer composites continues to expand because of their abundant availability, relatively low density, and potential to support the development of more environmentally friendly materials than synthetic reinforcements [1]-[4]. In Indonesia, sugar palm fiber derived from *Arenga pinnata* is an attractive lignocellulosic reinforcement because of its wide availability and potential for use in thermoset resin-based engineering materials. Interest in sugar palm fiber composites is increasing in response to the growing demand for lightweight materials derived from local resources while maintaining adequate mechanical performance and physical stability.

However, incorporating natural fibers into an unsaturated polyester matrix does not automatically produce composites with stable properties. The main challenge arises from the inherent mismatch between the two phases. Lignocellulosic fibers are hydrophilic because of their abundant hydroxyl groups, whereas unsaturated polyesters are relatively hydrophobic. This mismatch can reduce interfacial adhesion, hinder load transfer from the matrix to the fibers, increase the likelihood of void formation around the fibers, and increase the material's sensitivity to moisture [5], [6]. In many natural fiber composites, these effects are reflected not only in reduced reinforcement efficiency but also in higher water absorption and changes in internal structural characteristics as fiber content increases [7]-[9].

Various chemical treatments have been applied to improve fiber surface characteristics and enhance compatibility with polymer matrices. Alkalization is commonly used to remove surface impurities, partially dissolve hemicellulose and lignin, and increase fiber surface roughness. Silanization, by contrast, is used to improve interphase bonding by forming a more compatible layer between the fiber and the matrix [10]-[12]. However, the effectiveness of these treatments depends strongly on the fiber type, resin system, and reinforcement content employed. In other words, the success of surface modification cannot be assumed to be uniform across all natural fiber composite systems.

In a study by the author's team published in 2025, sugar palm fiber–polyester composites treated with 2% NaOH at fiber contents of 0–20 wt.% showed improvements in certain mechanical properties, but these improvements were not accompanied by a consistent increase in flexural strength at higher fiber contents [13]. These findings indicate that increasing fiber loading alone is insufficient to achieve effective reinforcement when fiber–matrix interfacial quality remains limited. Therefore, the key issue in sugar palm fiber–polyester composite systems lies not only in the amount of fiber added, but also in how the interface is engineered to better sustain stress transfer, structural stability, and moisture resistance [14]-[16].

In this context, the use of silane coupling agents such as Vinyltrimethoxysilane (VTMS) warrants further investigation [17], [18]. Conceptually, VTMS can function as an interphase linker because its silane groups interact with the hydroxyl groups on the fiber surface. In contrast, the vinyl groups have the potential to increase compatibility with the polyester matrix during curing [17], [18]. Here, VTMS is considered a plausible interfacial modifier rather than direct proof of a specific chemical mechanism.

Accordingly, combined alkali and VTMS treatment is expected not only to improve flexural strength but also to reduce water absorption and promote a more compact composite structure. However, in the sugar palm fiber–UPR composite system, the effect of this advanced interfacial treatment has not yet been adequately clarified through direct comparison among untreated fiber, alkali-treated fiber, and alkali–VTMS-treated fiber, particularly over a wider range of fiber contents and with respect to physical parameters related to internal structure.

Against this background, the present study examines whether interface engineering through combined alkali and VTMS treatment can deliver better composite properties than untreated and alkali-only conditions at fiber contents up to 50 wt.%. The specific contribution of this study lies in the comparative evaluation of three fiber treatment conditions, namely IU/UPR, IA/UPR, and IAS/UPR, at fiber contents of 0, 10, 20, 30, 40, and 50 wt.%, as well as in examining the relationship between flexural and physical properties, including hardness, water absorption, density, and porosity. Accordingly, this study evaluates the effects of fiber surface treatment and fiber content on the flexural properties and physical stability of sugar palm fiber-reinforced unsaturated polyester biocomposites, with emphasis on the role of interface modification.

2 Research methodology

2.1 Materials

The materials used in this study were type 235 polyester resin obtained from a local supplier in Bitung City, Mepoxy catalyst from PT Justus, sugar palm fiber collected from the North Sulawesi region, NaOH, VTMS as the silane coupling agent, ethanol, distilled water, and acetic acid. The sugar palm fiber was obtained

from sugar palm trees, cut to a length of approximately 15–20 cm, washed, and dried before further treatment.

2.2 Alkali and VTMS treatment of sugar palm fiber

The specimens were divided into three groups: untreated sugar palm fiber composites (IU/UPR), NaOH-treated sugar palm fiber composites (IA/UPR), and NaOH + VTMS-treated sugar palm fiber composites (IAS/UPR). For the untreated composites, cleaned sugar palm fibers were used without further chemical treatment. For the alkali-treated fibers, sugar palm fibers were immersed in a 2 wt.% NaOH solution at 70°C for 1 hour, with a fiber-to-solution ratio of 1:20 (w/v). The fibers were then rinsed repeatedly until a neutral pH was reached and dried in an oven at 60°C for 24 hours [19], [20].

For the IAS/UPR composites, the alkali treatment was followed by silanization using 1 wt.% VTMS. The VTMS solution was prepared in an ethanol: water solvent system at a 60:40 (v/v) ratio, and the pH was adjusted to 4.5–5.0 with acetic acid. The solution was stirred for 30 minutes, after which the fibers were immersed for 45 minutes at room temperature [17], [18]. After immersion, the fibers were rinsed with ethanol to remove any residual unbound silane, dried again at 80°C for 24 hours, and stored under dry conditions before use.

2.3 Preparation of sugar palm fiber composites

The composites were prepared from untreated, alkali-treated, and alkali–VTMS-treated sugar palm fibers using an unsaturated polyester resin matrix. For ease of discussion, the untreated composite is referred to as IU/UPR, the NaOH-treated composite as IA/UPR, and the alkali–VTMS-treated composite as IAS/UPR. Fiber contents of 0, 10, 20, 30, 40, and 50 wt.% were used, as summarized in Table 1. The fibers were aligned in the same direction within the mold, and the composites were fabricated using the hand lay-up method [14], [20], [21].

Unidirectional alignment was selected to promote more consistent load transfer along the specimen length during flexural testing and to reduce variability caused by random fiber orientation.

The composites were cured in stages. Initial gelation was carried out at room temperature (25–30°C) for 3–4 hours, followed by curing I at 70°C for 45 minutes, curing II at 90°C for 60 minutes, and post-curing at 100°C for 60–90 minutes. Cooling was performed gradually in the oven until the temperature dropped below 40°C [20]-[23].

Table 1. Composition of sugar palm fiber composite specimens

Specimen type	Specimen code	Fiber content (wt.%)
Untreated	UPR-0	0
	IU/UPR-10	10
	IU/UPR-20	20
	IU/UPR-30	30
	IU/UPR-40	40
	IU/UPR-50	50
NaOH-treated	IA/UPR-10	10
	IA/UPR-20	20
	IA/UPR-30	30
	IA/UPR-40	40
	IA/UPR-50	50
NaOH + VTMS treated	IAS/UPR-10	10
	IAS/UPR-20	20
	IAS/UPR-30	30
	IAS/UPR-40	40
	IAS/UPR-50	50

2.4 Material testing

Flexural testing was conducted using the three-point bending method in accordance with ASTM D790. Hardness was measured using the Shore D method according to ASTM D2240. Water absorption was determined according to ASTM D570 using a 24-hour immersion test. Density was measured based on Archimedes' principle in accordance with ASTM D792 [24]. The overall treatment and fabrication scheme for the sugar palm fiber composites is presented in Fig. 1.

Fig. 1. Schematic illustration of alkali–VTMS treatment of sugar palm fiber and composite fabrication.

The flexural test specimens were prepared as rectangular beams with dimensions of 127×12.7×3.2 mm³ and tested in a three-point bending configuration using a support span of 51 mm and a crosshead speed of 2 mm/min. For Shore D hardness testing, measurements were taken at five different points on each specimen, and the reported value represents the average of those measurements.

Water absorption testing was carried out on specimens measuring 76×25×3 mm³. The specimens were first dried to constant mass, and then immersed in distilled water at 23°C for 24 hours according to ASTM D570. After immersion, the specimen surface was dried with lint-free tissue before reweighing. Water absorption was calculated using Eq. (1), where W_A is the water absorption, W_1 is the mass before immersion, and W_2 is the mass after immersion.

$$W_A(\%) = \frac{W_2 - W_1}{W_1} \times 100 \quad (1)$$

The experimental density was determined by the Archimedes method according to ASTM D792, using distilled water as the testing medium at 28°C (room temperature). The density of the composite was calculated using the weight of the specimen in air and in water, as shown in Eq. (2), where W_{air} and W_{water} are the masses of the specimen in air and when immersed in water, respectively, ρ_{water} is the density of water, and ρ is the density of the composite.

$$\rho = \frac{W_{air}}{W_{air} - W_{water}} \times \rho_{water} \quad (2)$$

Porosity was then calculated using Eq. (3), where ρ_t is the theoretical density and ρ_e is the experimental density.

$$\text{Porosity } (\%) = \frac{\rho_t - \rho_e}{\rho_t} \times 100 \quad (3)$$

The theoretical density was calculated using Eq. (4), where W_f is the weight fraction of fiber, W_m is the weight fraction of matrix, ρ_f is the density of fiber, and ρ_m is the density of the matrix.

$$\rho_{theo} = \frac{1}{\frac{W_f}{\rho_f} + \frac{W_m}{\rho_m}} \quad (4)$$

Each test was conducted on three independent specimens for each composition. The values reported in the tables are presented as mean ± standard deviation (n = 3). For hardness testing, the value for each specimen was obtained by averaging five-point measurements, followed by averaging across the specimens.

2.5 Statistical analysis

All experimental data were expressed as mean ± standard deviation. Statistical analysis was performed using two-way Analysis of Variance (ANOVA) to evaluate the effects of fiber treatment, fiber loading, and their interaction on flexural strength, hardness, water absorption, density, and porosity. The significance level was set at $p < 0.05$. When significant effects were detected, Tukey's Honestly Significant Difference (HSD) test was used as a post-hoc comparison to identify differences among treatment groups. Statistical analysis was performed based on the raw experimental data obtained from three independent specimens for each composite composition.

2.6 FTIR characterization

Fourier-Transform Infrared Spectroscopy (FTIR) was used to identify changes in the functional groups of sugar palm fibers after alkali and alkali–VTMS treatments. The FTIR analysis was performed using a Thermo Scientific Nicolet iS10 FTIR spectrometer over a wavenumber range of 4000–500 cm^{-1}. The spectra of untreated, NaOH-treated, and NaOH–VTMS-treated sugar palm fibers were compared to evaluate changes in hydroxyl groups, lignocellulosic components, and silane-related bonding features. The FTIR results were used to support the interpretation of fiber surface modification and interfacial compatibility [25].

2.7 SEM observation

Scanning Electron Microscopy (SEM) was carried out to observe the morphological features of the composite fracture surfaces and the fiber–matrix interfacial region. SEM observation was performed on the 50 wt.% fiber-loaded composites, namely IU/UPR-50, IA/UPR-50, and IAS/UPR-50, because this fiber loading represented the highest reinforcement content and showed the most distinct differences in flexural and physical properties among the three treatment systems. The fractured surfaces of IU/UPR, IA/UPR, and IAS/UPR composites were cut into suitable dimensions, dried, mounted on specimen stubs, and coated with Au/Pd before observation. SEM images were obtained using a Philips XL30 SEM microscope operated at an accelerating voltage of 15 kV. The SEM observations were used to compare fiber pull-out, interfacial gaps, void formation, matrix cracking, resin wetting, and fiber–matrix adhesion among the untreated, NaOH-treated, and NaOH–VTMS-treated composites [26].

3 Results and discussion

The two-way ANOVA results confirmed that the measured composite properties were influenced by both fiber treatment and fiber loading. Treatment, fiber loading, and their interaction significantly affected flexural strength, water absorption, and porosity ($p < 0.05$). For hardness and density, the main effects of treatment and fiber loading were significant, whereas the interaction between the two was not significant. These results indicate that the effect of alkali–VTMS treatment was property-dependent: it produced a strong interaction effect for properties closely associated with reinforcement efficiency and internal structure, while hardness and density were mainly governed by the individual effects of treatment and fiber content. The summary of the two-way ANOVA results for each measured property is presented in Table 2.

Table 2. Summary of two-way ANOVA for the effects of treatment, fiber loading, and their interaction

Property	Treatment	Fiber loading	Treatment × loading
Flexural strength	Significant	Significant	Significant
Hardness	Significant	Significant	Not significant
Water absorption	Significant	Significant	Significant
Density	Significant	Significant	Not significant
Porosity	Significant	Significant	Significant

3.1 Effect of treatment and fiber content on flexural strength

The flexural test results clearly show that both fiber treatment and fiber loading strongly influenced the mechanical performance of the composites. At a given fiber content, the alkali–VTMS-treated composites (IAS/UPR) consistently exhibited the highest flexural strength, followed by the alkali-treated composites (IA/UPR) and the untreated composites (IU/UPR). This trend became apparent at 10 wt.% and became more pronounced as fiber loading increased. At 50 wt.%, for example, the flexural strength reached 37.20 MPa for IU/UPR, 50.60 MPa for IA/UPR, and 110.59 MPa for IAS/UPR. These results indicate that fiber addition can enhance flexural strength, but that reinforcement efficiency is strongly governed by fiber surface treatment, particularly at high fiber loadings.

Statistical analysis confirmed that flexural strength was significantly affected by fiber treatment, fiber loading, and their interaction ($p < 0.05$). The significant interaction indicates that the effect of fiber loading on flexural strength depends strongly on the

type of fiber treatment. This finding supports the observed trend in which IU/UPR and IA/UPR declined after 30 wt.% fiber loading, whereas IAS/UPR continued to increase up to 50 wt.%. Therefore, the superior flexural performance of IAS/UPR at high fiber loading cannot be attributed only to the amount of fiber added, but also to the effectiveness of alkali–VTMS treatment in maintaining reinforcement efficiency and stress transfer under fiber-rich conditions.

As shown in Table 3 and Fig. 2, IAS/UPR consistently delivered the highest flexural strength at each fiber content. Compared with untreated composites, alkali treatment improved flexural strength across the entire fiber-loading range, indicating that alkalization improved fiber surface condition and promoted more efficient stress transfer between the matrix and the reinforcement [16], [20]. The most pronounced improvement was observed in the IAS/UPR system. In this system, flexural strength was higher at all fiber contents and continued to increase up to 50 wt.%, whereas IU/UPR and IA/UPR showed declining trends beyond 30 wt.%. This pattern suggests that interfacial modification through the combined alkali–VTMS treatment is more effective at maintaining reinforcement efficiency at high fiber loadings.

Table 3. Flexural strength of sugar palm fiber composites

Fiber content (wt.%)	Flexural strength (MPa)		
	Untreated	NaOH	NaOH + VTMS
0	22.35 ± 1.12	22.35 ± 1.12	22.35 ± 1.12
10	28.90 ± 1.85	30.20 ± 3.12	31.76 ± 1.45
20	35.70 ± 1.60	44.80 ± 2.15	47.06 ± 2.08
30	40.91 ± 3.45	58.14 ± 3.52	62.35 ± 2.31
40	39.10 ± 3.22	55.20 ± 2.12	81.18 ± 2.76
50	37.20 ± 4.12	50.60 ± 0.77	110.59 ± 3.14

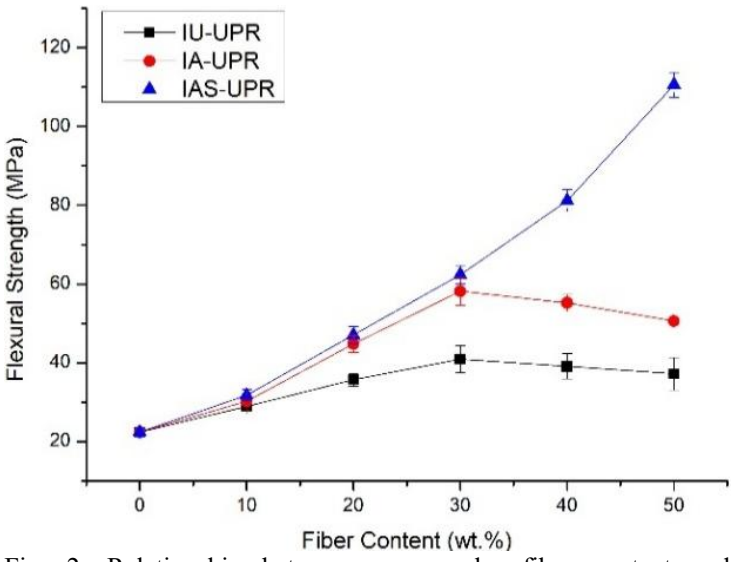

Fig. 2. Relationship between sugar palm fiber content and composite flexural strength.

The decrease in flexural strength of IU/UPR and IA/UPR after 30 wt.% fiber loading is attributed to reduced resin impregnation, fiber wetting, and stress transfer at higher fiber contents. This explanation is supported by Norizan *et al.* (2018), who investigated sugar palm yarn fiber-reinforced unsaturated polyester composites with fiber loadings of 10–50 wt.% prepared using the hand lay-up method and reported that fiber loading strongly influences the mechanical behavior of sugar palm fiber/polyester composites [16]. In the present study, the reduction in flexural strength of IU/UPR and IA/UPR at 40–50 wt.% indicates that the higher fiber population increased the interfacial area, restricted resin flow, and promoted void development, thereby reducing the efficiency of load transfer from the matrix to the fibers. Furthermore, Asyraf *et al.* (2022) reported that the hydrophilic nature of sugar palm fiber increases moisture uptake and inhibits effective bonding between the fiber and polymer matrix; therefore, chemical treatment is required to improve fiber–matrix interaction [27]. Based on this theory, the lower performance of IU/UPR is associated with weak compatibility between untreated sugar palm fiber and the hydrophobic UPR matrix, whereas the decrease in IA/UPR after 30 wt.% indicates that alkali treatment alone is not sufficient to maintain effective interfacial bonding at high fiber loading.

In contrast, the continuous increase in flexural strength of IAS/UPR up to 50 wt.% fiber loading demonstrates that the combined alkali–VTMS treatment was more effective in maintaining reinforcement efficiency under high fiber content conditions. This behavior is explained by the complementary role of alkali and silane treatments. Alkali treatment removes surface impurities and increases fiber surface roughness, whereas VTMS acts as a coupling agent that improves the compatibility between the hydrophilic sugar palm fiber surface and the hydrophobic UPR matrix. This interpretation is supported by Atiqah *et al.* (2018), who investigated silane-treated sugar palm fiber-reinforced polymer composites at fiber loadings of 0–50 wt.% and reported that silane treatment improved the fiber–matrix interface, with SEM observations showing good bonding and linkage between cellulose fibers and the polymer matrix, thereby contributing to improved mechanical properties [17]. Similarly, Srinivasan *et al.* (2025) reported that combined alkali–silane treatment in natural fiber-reinforced polymer biocomposites enhances fiber–matrix bonding, removes impurities, reduces hydrophilic surface groups, and improves load transfer [30]. Therefore, in the present IAS/UPR system, the continuous increase in flexural strength from 30 to 50 wt.% is associated with better resin impregnation, stronger interfacial compatibility, lower void development, and more effective stress transfer compared with IU/UPR and IA/UPR. This explanation is consistent with the porosity results, where IAS/UPR showed lower porosity than IU/UPR and IA/UPR at the same fiber loading.

3.2 Effect of treatment and fiber content on hardness

In contrast to flexural strength, composite hardness remained within a relatively narrow range of 85.9–87.1 Shore D. At all fiber contents, the differences among IU/UPR, IA/UPR, and IAS/UPR were small, indicating that fiber surface treatment and increasing fiber fraction did not markedly alter surface hardness. In other words, hardness was not the most sensitive parameter for capturing the effect of interfacial modification in this system.

The two-way ANOVA showed that treatment and fiber loading had significant effects on hardness ($p<0.05$), whereas their interaction was not significant. Although the statistical results indicate measurable differences among treatment and loading conditions, the absolute hardness variation remained small. Therefore, hardness should be interpreted carefully as a secondary indicator of surface stability rather than as direct evidence of interfacial strengthening. The absence of a significant interaction also suggests that the effect of alkali–VTMS treatment on hardness was not strongly dependent on fiber loading.

The hardness values of the composites at different fiber contents and treatment conditions are presented in Table 4 and illustrated in Fig. 3.

Table 4. Hardness of sugar palm fiber composites

Fiber content (wt.%)	Hardness (Shore D)		
	Untreated	NaOH	NaOH + VTMS
0	86.6 ± 0.20	86.6 ± 0.20	86.6 ± 0.20
10	86.4 ± 0.11	86.8 ± 0.17	87.1 ± 0.15
20	86.1 ± 0.13	86.4 ± 0.21	86.6 ± 0.18
30	85.9 ± 0.20	86.2 ± 0.09	86.5 ± 0.17
40	86.1 ± 0.09	86.5 ± 0.16	86.8 ± 0.21
50	86.0 ± 0.15	86.4 ± 0.17	86.8 ± 0.19

Although the differences in hardness were limited, this parameter remains relevant because it shows that increasing the fiber content up to 50 wt.% did not cause severe surface

degradation. In the IAS/UPR system, hardness values tended to be slightly higher and more stable than those of the other two groups, but the differences were not large enough to support strong claims regarding improved interfacial quality. Accordingly, hardness is better interpreted here as an indicator of surface stability rather than as primary evidence for the effectiveness of alkali–VTMS treatment.

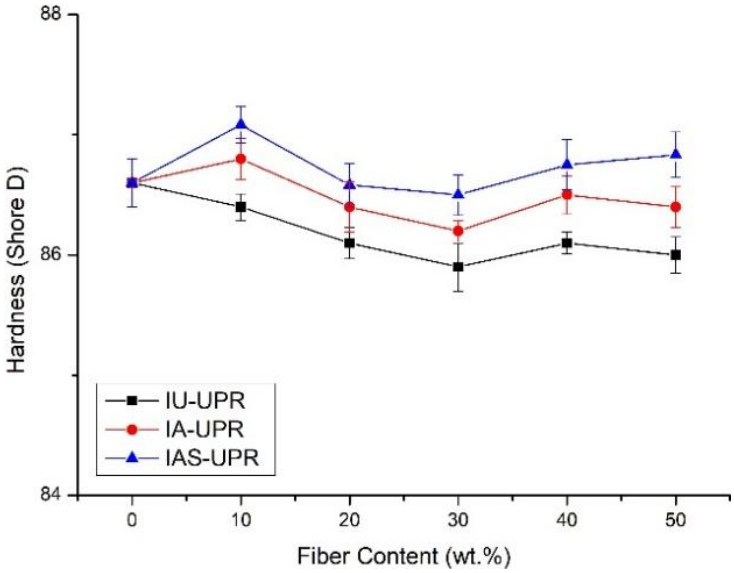

Fig. 3. Relationship between sugar palm fiber content and composite hardness.

This finding is consistent with the limited sensitivity of hardness to interfacial modification in this system. In natural fiber composites, hardness can be influenced by matrix stiffness, local fiber distribution, impregnation quality, and surface homogeneity. Because these factors overlap, the relatively stable hardness values observed across the three treatment systems more reasonably indicate that the manufacturing process produced fairly uniform composite surfaces, even though this parameter is not sufficiently robust to explain interphase mechanisms in detail.

3.3 Effect of treatment and fiber content on water absorption

Water absorption increased with increasing fiber content in all three composite systems. This trend is reasonable because the addition of lignocellulosic fiber increases the surface area available for water interaction [27]. More importantly, however, IAS/UPR consistently showed the lowest water absorption at each fiber content, followed by IA/UPR and then IU/UPR. At 50 wt.%, water absorption reached 5.22% in IU/UPR, 3.91% in IA/UPR, and 3.45% in IAS/UPR. Thus, although alkali–VTMS treatment did not eliminate the increase in water absorption associated with higher fiber loading, it consistently reduced its magnitude.

The water absorption values for IU/UPR, IA/UPR, and IAS/UPR composites are presented in Table 5, while the corresponding trend is shown in Fig. 4.

Table 5. Water absorption value of sugar palm fiber composites

Fiber content (wt.%)	Water absorption (%)		
	Untreated	NaOH	NaOH + VTMS
0	0.29 ± 0.03	0.29 ± 0.03	0.29 ± 0.03
10	1.36 ± 0.09	1.24 ± 0.08	1.14 ± 0.07
20	1.79 ± 0.30	1.63 ± 0.11	1.50 ± 0.09
30	2.78 ± 0.21	2.46 ± 0.10	2.23 ± 0.12
40	4.54 ± 0.13	3.86 ± 0.25	2.90 ± 0.15
50	5.22 ± 0.11	3.91 ± 0.18	3.45 ± 0.18

The two-way ANOVA confirmed that water absorption was significantly affected by treatment, fiber loading, and their interaction ($p < 0.05$). The significant interaction indicates that the ability of the treatment to suppress water absorption became more evident as fiber loading increased. This result is consistent with the sharper increase in water absorption observed in IU/UPR compared with IA/UPR and IAS/UPR at higher fiber contents. The lower water absorption of IAS/UPR suggests that alkali–VTMS treatment reduced moisture-sensitive pathways by improving fiber–matrix compatibility and limiting interfacial voids.

This pattern supports the hypothesis that fiber surface modification reduces the moisture sensitivity of the composites. Alkalization helps clean the fiber surface, while VTMS reduces the effective hydrophilic character at the interface and improves structural homogeneity [17], [18], [28].

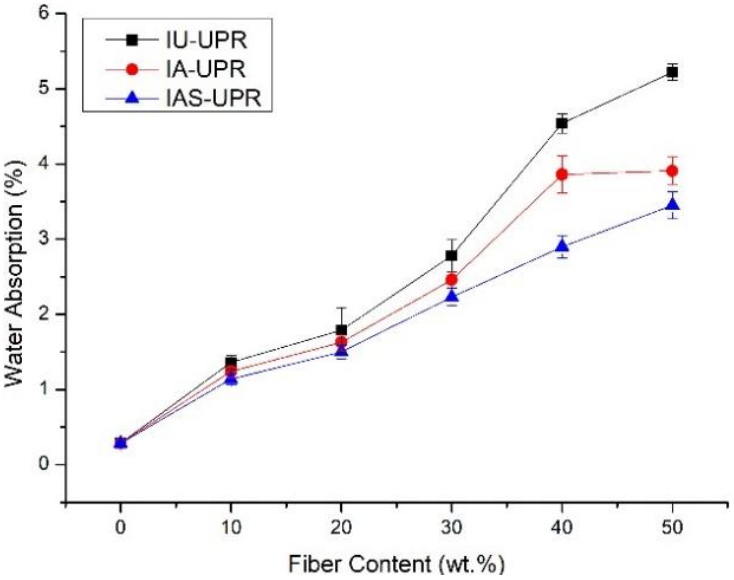

Fig. 4. Relationship between sugar palm fiber content and composite water absorption.

Table 5 and Fig. 4 show that the alkali–VTMS-treated composites maintained lower water absorption even at a fiber loading of 50 wt.%. This is notable because, in many natural fiber composites, higher fiber fractions are accompanied by a marked rise in water absorption [28], [29]. In the present study, the IAS/UPR system showed that increasing fiber content did not produce as sharp an increase in water absorption as that observed in IU/UPR and IA/UPR. These data therefore support the view that interfacial modification influences not only flexural response but also the physical stability of the composites under humid conditions.

3.4 Effect of treatment and fiber content on density

The density results showed that composite density increased with fiber content for all treatments. In addition, at a given fiber loading, density consistently followed the order IAS/UPR > IA/UPR > IU/UPR. At 50 wt.%, the densities were 1.15 g/mL for IU/UPR, 1.20 g/mL for IA/UPR, and 1.25 g/mL for IAS/UPR. This trend indicates that fiber surface modification is associated with the formation of a denser composite structure in the more advanced treatment systems.

Statistical analysis showed that density was significantly affected by treatment and fiber loading ($p<0.05$), but the interaction between the two was not significant. This result indicates that both the type of fiber treatment and the amount of fiber contributed to changes in composite density, but their combined effect was not strong enough to yield a statistically significant interaction. Therefore, the higher density of IAS/UPR should be interpreted as a general consequence of improved packing and matrix filling associated with alkali–VTMS treatment, rather than as a fiber-loading-dependent interaction effect.

The density values of the composites as a function of fiber content and treatment condition are presented in Table 6 and plotted in Fig. 5. The increase in density can be attributed to two factors. First, increasing fiber content increases the composite's

solid fraction. Second, the density differences among the treatment systems suggest that matrix filling around the fibers became more effective in IA/UPR and, especially, in IAS/UPR. Accordingly, density may be considered a structural indicator of improved interfacial compatibility.

Table 6. Density of sugar palm fiber composites

Fiber content (wt.%)	Density (g/mL)		
	Untreated	NaOH	NaOH + VTMS
0	1.11 ± 0.02	1.11 ± 0.02	1.11 ± 0.02
10	1.12 ± 0.01	1.13 ± 0.02	1.14 ± 0.02
20	1.13 ± 0.02	1.14 ± 0.03	1.15 ± 0.03
30	1.13 ± 0.02	1.15 ± 0.02	1.16 ± 0.02
40	1.14 ± 0.01	1.18 ± 0.03	1.22 ± 0.03
50	1.15 ± 0.03	1.20 ± 0.02	1.25 ± 0.03

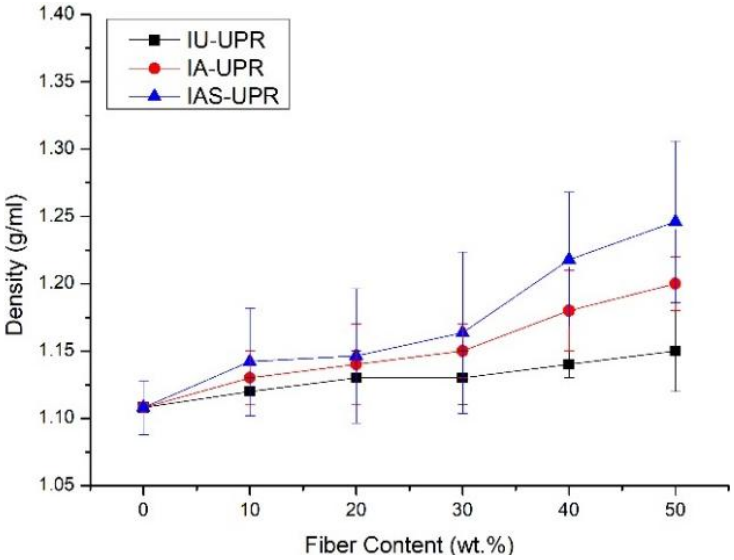

Fig. 5. Relationship between sugar palm fiber content and composite density.

However, higher density should not be interpreted as evidence that the composite is free of voids. The density data in Table 6 must be considered together with the porosity results in Table 7. In this system, density increased with fiber content, but porosity also increased. This indicates that the composite structure became denser as fiber fraction increased, while the likelihood of microvoid formation also rose. Therefore, density should be interpreted within the broader context of structural behavior rather than as an isolated parameter.

3.5 Effect of treatment and fiber content on porosity

Porosity increased with increasing fiber content in all composite systems. This can be understood as a consequence of the larger interfacial area and the more complex resin flow during hand lay-up and curing. More importantly, at the same fiber content, IAS/UPR consistently exhibited the lowest porosity, followed by IA/UPR and IU/UPR. At 50 wt.%, porosity reached 18.31% in IU/UPR, 15.75% in IA/UPR, and 14.61% in IAS/UPR. Thus, fiber surface treatment did not completely prevent void formation, but it was clearly associated with lower porosity than in the untreated and alkali-only systems.

The two-way ANOVA indicated that porosity was significantly affected by treatment, fiber loading, and their interaction ($p<0.05$). The significant interaction suggests that the effect of fiber loading on porosity differed among the three treatment systems. Although porosity increased with increasing fiber content in all composites, the increase was less severe in IAS/UPR than in IU/UPR and IA/UPR. This result supports the interpretation that alkali–VTMS treatment improved wetting and matrix filling around the fibers, thereby reducing void development, particularly at higher fiber loadings. The porosity values of the composites with different fiber contents and treatment conditions are presented in Table 7, and the corresponding trends are shown in Fig. 6.

Table 7. Porosity of sugar palm fiber composites

Fiber content (wt.%)	Porosity (%)		
	Untreated	NaOH	NaOH + VTMS
0	4.13 ± 0.21	4.13 ± 0.21	4.13 ± 0.21
10	7.42 ± 0.13	7.18 ± 0.27	6.95 ± 0.34
20	11.12 ± 0.61	9.56 ± 0.45	8.17 ± 0.40
30	13.10 ± 0.82	12.30 ± 0.32	11.79 ± 0.52
40	14.85 ± 0.35	13.82 ± 0.54	12.90 ± 0.58
50	18.31 ± 0.55	15.75 ± 0.12	14.61 ± 0.63

The porosity trend should be considered together with the simultaneous increases in density and flexural strength. Although porosity increased at higher fiber loadings, the increase was gradual and should be considered alongside the simultaneous increases in density and improvement in flexural strength. This combined pattern suggests that the voids formed were more likely dispersed microvoids than macro-defects that directly impaired composite properties. Accordingly, the porosity results are better interpreted not as evidence of processing failure, but as an indication of the practical limits of fiber packing, particularly at 40–50 wt.%.

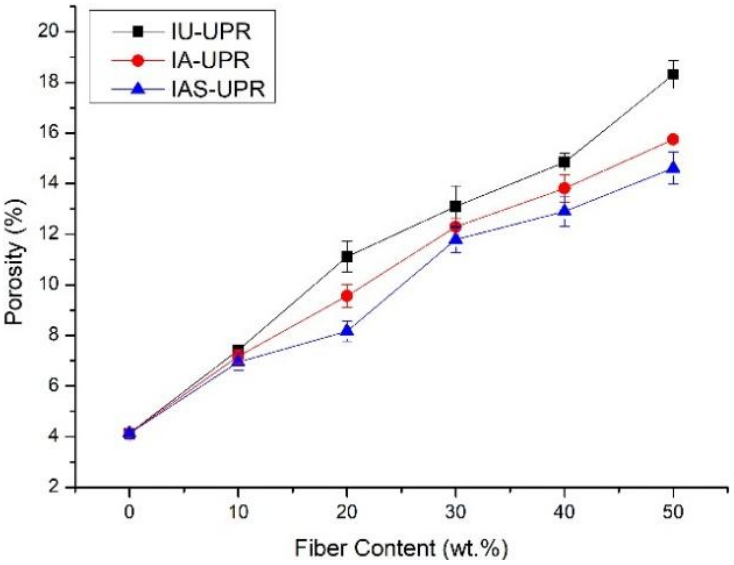

Fig. 6. Relationship between sugar palm fiber content and composite porosity.

Structurally, the increase in porosity at high fiber loadings is due to fiber crowding, in which a high fiber population begins to interfere with uniform resin distribution. Nevertheless, the lower porosity of IAS/UPR relative to IA/UPR and IU/UPR suggests that alkali–VTMS modification likely improved wetting and matrix filling at the interface. Although not direct evidence of an interfacial mechanism, this pattern is consistent with improved structural compatibility.

3.6 FTIR analysis of treated sugar palm fibers

The FTIR spectra of untreated, NaOH-treated, and NaOH–VTMS-treated sugar palm fibers are shown in Fig. 7. The broad absorption band around 3307 cm^{-1} is associated with O–H stretching vibration from hydroxyl groups in cellulose, hemicellulose, and lignin. The absorption bands at approximately 2907 and 2867 cm^{-1} correspond to asymmetric and symmetric C–H stretching vibrations, respectively. In the untreated fiber, the band around 1730 cm^{-1} is attributed to C=O stretching of hemicellulose, whereas the bands near 1600 and 1510 cm^{-1} are related to aromatic lignin vibrations. The band at approximately 1186 cm^{-1} is associated with C–O vibration of lignin and hemicellulose-related components, while the band around 1030 cm^{-1} is mainly assigned to C–O stretching in the cellulose-rich region. The band at 895 cm^{-1} indicates β-glycosidic linkage in the cellulose structure.

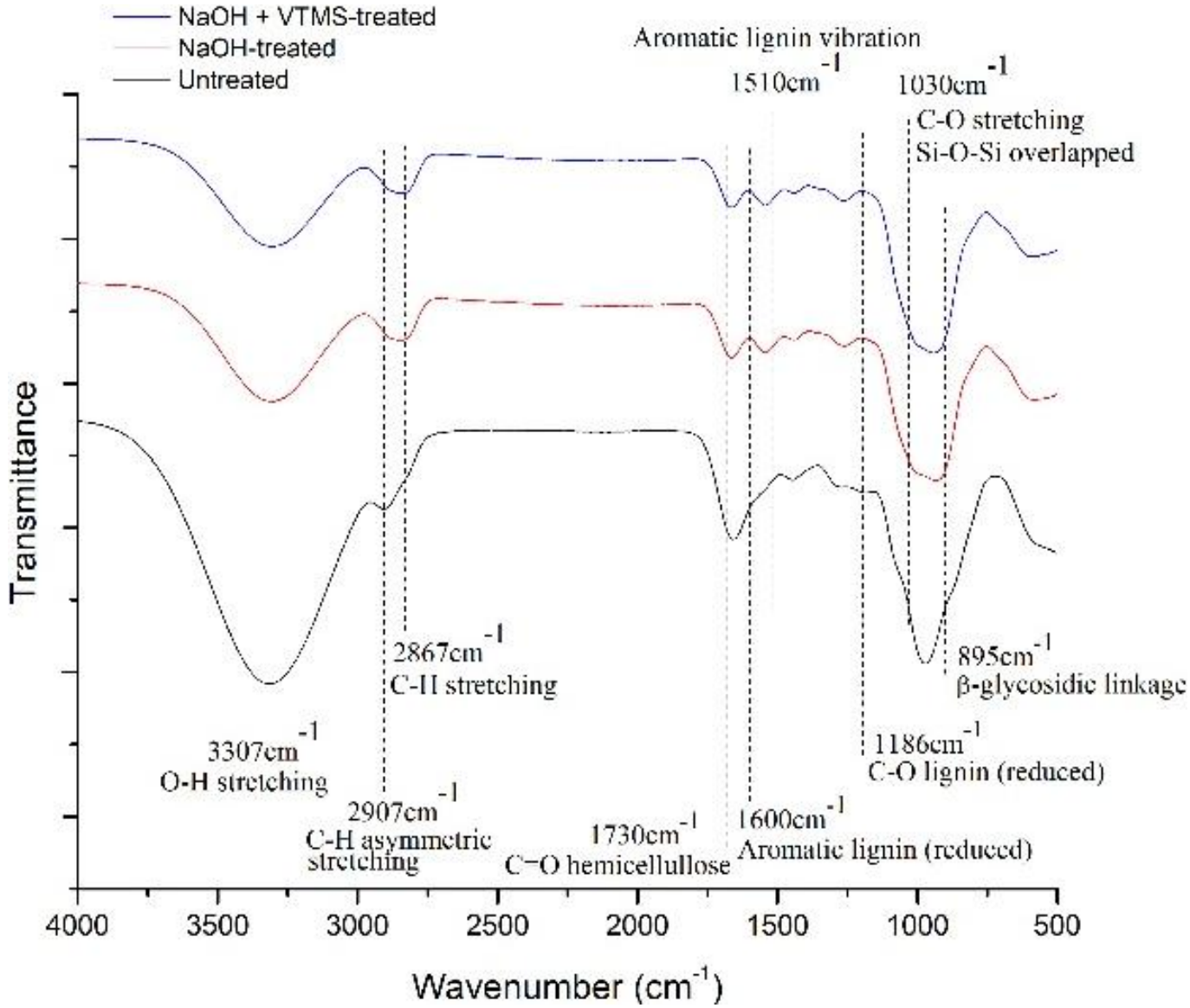

Fig. 7. FTIR spectra of untreated, NaOH-treated, and NaOH–VTMS-treated sugar palm fibers showing changes in functional groups after surface modification.

After NaOH treatment, the intensity of several absorption bands associated with hemicellulose and lignin decreased particularly those around 1730, 1600, 1510, and 1186 cm^{-1}. The reduction of the 1730 cm^{-1} band indicates the partial removal of hemicellulose, while the decrease in the bands around 1600, 1510, and 1186 cm^{-1} suggests the reduction of lignin-related aromatic and C–O vibrations. These changes indicate that alkali treatment removed part of the non-cellulosic components, waxes, and surface impurities from the sugar palm fiber. Such removal is important because it exposes a cleaner cellulose-rich surface and can increase the accessibility of the fiber surface for further modification.

For the NaOH–VTMS-treated fiber, the most relevant spectral change is observed in the fingerprint region around 1030 cm^{-1}. This band is mainly associated with C–O stretching of cellulose; however, in the NaOH–VTMS-treated fiber, this region may also overlap with Si–O–Si or Si–O–C vibrations associated with silane treatment. Therefore, the FTIR result is interpreted as supporting evidence of surface modification after NaOH–VTMS treatment, rather than definitive proof of an isolated Si–O interfacial layer. The absence of a clearly separated Si–O peak indicates that the silane-related contribution may be weak or overlapped with the strong lignocellulosic C–O band in this region.

FTIR spectra indicate that NaOH treatment reduced hemicellulose and lignin-related components, while subsequent VTMS treatment further modified the chemical environment of the fiber surface, particularly in the cellulose-rich fingerprint region. This chemical evidence supports the interpretation that the combined NaOH–VTMS treatment reduced the hydrophilic character of the fiber surface and improved its compatibility with the unsaturated polyester matrix. These changes are consistent with the lower water absorption, lower porosity, and higher flexural strength observed in the IAS/UPR composites compared with the IU/UPR and IA/UPR composites.

3.7 SEM morphology of fiber–matrix interface

SEM micrographs of 50 wt.% fiber-loaded IU/UPR, IA/UPR, and IAS/UPR composites are shown in Fig. 8. The untreated composite (IU/UPR) showed visible fiber pull-out, interfacial gaps, voids, and matrix cracking, indicating weak adhesion between the hydrophilic sugar palm fiber and the hydrophobic UPR matrix. The NaOH-treated composite (IA/UPR) exhibited improved fiber–matrix contact with fewer interfacial gaps than IU/UPR. This improvement is attributed to the removal of surface impurities, hemicellulose, waxes, and part of the lignin during alkali treatment, which produced a cleaner and rougher fiber surface for better mechanical interlocking.

The NaOH–VTMS-treated composite (IAS/UPR) showed the most compact interfacial morphology, with better matrix coverage, fewer visible gaps, and reduced fiber pull-out. This morphology indicates improved resin wetting and stronger fiber–matrix adhesion after the combined NaOH–VTMS treatment. The SEM observations support the FTIR and statistical results, showing that alkali–VTMS treatment improved interfacial compatibility. This improved interface helps explain the higher flexural strength, lower water absorption, higher density, and lower porosity of IAS/UPR compared with IU/UPR and IA/UPR.

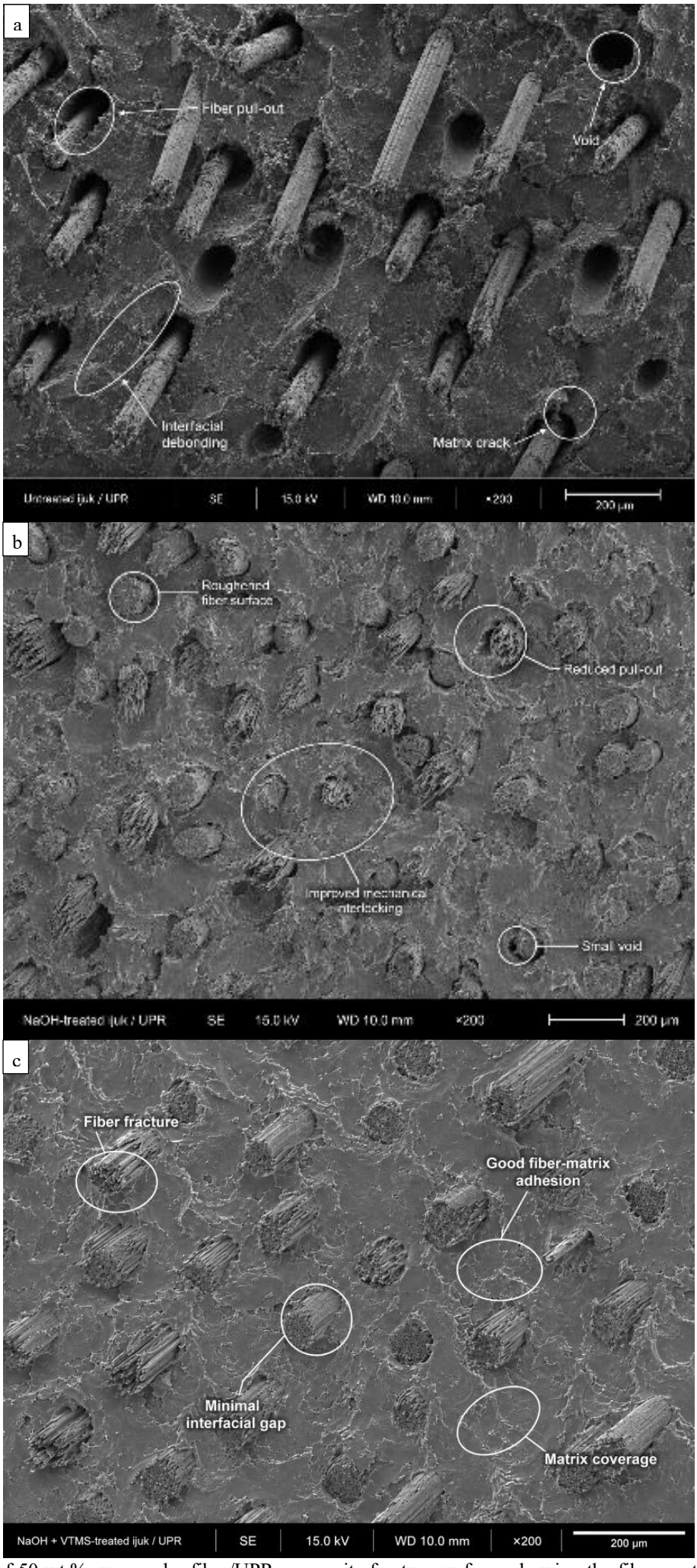

Fig. 8. SEM micrographs of 50 wt.% sugar palm fiber/UPR composite fracture surfaces showing the fiber–matrix interfacial morphology: (a) IU/UPR-50, (b) IA/UPR-50, and (c) IAS/UPR-50.

3.8 Integrated interfacial mechanism

When the results are considered collectively, alkali–VTMS treatment produced the most consistently favorable performance among the three composite systems. At a given fiber content, IAS/UPR exhibited the highest flexural strength, the lowest water absorption, the highest density, and the lowest porosity, while hardness remained within a stable range. The two-way ANOVA also confirmed that treatment, fiber loading, and their interaction significantly affected flexural strength, water absorption, and porosity. These findings indicate that the superior performance of IAS/UPR was not due solely to fiber addition, but to the combined effects of fiber loading and improved interfacial compatibility.

The FTIR results indicate that NaOH treatment reduced hemicellulose and lignin-related components, while NaOH–VTMS treatment further modified the chemical environment of the fiber surface, particularly in the cellulose-rich fingerprint region. Although the possible silane-related band overlaps with lignocellulosic C–O vibrations, the spectral changes support the occurrence of surface modification after chemical treatment. This chemical modification is consistent with the lower water absorption of IAS/UPR, suggesting reduced moisture-sensitive pathways in the composite.

The SEM observations provide microstructural support for this interpretation. Compared with IU/UPR and IA/UPR, the IAS/UPR composite showed better matrix coverage, fewer visible interfacial gaps, and reduced fiber pull-out. These features indicate improved resin wetting and stronger fiber–matrix adhesion. Therefore, the improved flexural response of IAS/UPR can be attributed to more effective stress transfer. At the same time, its lower porosity and higher density indicate better matrix filling and reduced void formation at the interface.

Overall, the combined statistical, FTIR, and SEM results support the proposed mechanism that alkali treatment cleans and roughens the fiber surface, while VTMS treatment improves compatibility between sugar palm fiber and the UPR matrix. This integrated mechanism explains why IAS/UPR maintained superior performance even at 50 wt.% fiber loading. The main contribution of this study is therefore the demonstration that alkali–VTMS interface engineering can extend the effective fiber-loading range of sugar palm fiber/UPR biocomposites.

4 Conclusions

This study evaluates the role of alkali–VTMS treatment as an interfacial modification strategy for high-loading sugar palm fiber/UPR biocomposites. Based on the experimental results, several conclusions can be drawn: (1) Combined alkali–VTMS treatment improved the overall performance of sugar palm fiber/UPR biocomposites. Across the fiber-loading range of 0–50 wt.%, IAS/UPR showed better performance than IU/UPR and IA/UPR. Physical properties were also improved by the combined treatment. IAS/UPR showed lower water absorption, higher density, and lower porosity than untreated and alkali-treated composites; (2) Statistical analysis confirmed the significance of treatment and fiber loading. Fiber treatment, fiber loading, and their interaction significantly affected flexural strength, water absorption, and porosity, while hardness and density were influenced mainly by the individual factors; (3) Microstructural and chemical analyses support the interfacial improvement mechanism. FTIR indicated the reduction of hemicellulose and lignin components, while SEM showed improved matrix coverage, fewer interfacial gaps, and reduced fiber pull-out. Future studies should include interfacial and durability analyses to further validate the bonding mechanism.

Acknowledgment

The authors would like to express their sincere gratitude to Politeknik Kelautan dan Perikanan Bitung as the research site and to all parties who provided assistance, input, and constructive suggestions during the preparation of this manuscript.

References

[1] C. Iswan, B. Maryanti, and K. Arifin, “Analisis Perbandingan Kekuatan Variasi Fraksi Volume Komposit Serat Ijuk Terhadap Sifat Mekanis Komposit Dengan Matriks Resin Epoksi,” presented at the SNITT- Politeknik Negeri Balikpapan 2018, 2018.

[2] D. A. Ramadhan, F. Putri, and D. Arnoldi, “Analisis Ketangguhan Material Alternatif Komposit Serat Ijuk dan Resin Polyester Sebagai Cover Body Motor,” Jun. 2021, doi: 10.5281/ZENODO.5812356.

[3] Laily Ulfiyah, Faizatur Rohmah, Tristiandinda Permata, and Yopi Ariyanto, “Analisa Sifat Mekanik Paduan Serat Ijuk Dan Serat Jerami Sebagai Pengganti Serat Sintetis Pada Body Mobil,” *J. Rekayasa Mater. Manufaktur Dan Energi*, vol. 4, no. 2, Sep. 2021, doi: 10.30596/rmme.v4i2.8072.

[4] R. D. Widodo, F. A. N. Susetyo, R. Rusiyanto, K. Kriswanto, and F. B. Darsono, “Kekuatan Tarik dan Bending Komposit Berpenguat Serat Arengga Pinnata Bermatriks Epoksi Berbasis Fraksi Volume dan Orientasi Serat,” *Media Mesin Maj. Tek. Mesin*, vol. 23, no. 1, pp. 1–12, Jan. 2022, doi: 10.23917/mesin.v23i1.15791.

[5] A. Karthik, M. Bhuvaneshwaran, M. S. Senthil Kumar, S. Palanisamy, M. Palaniappan, and N. Ayrilmis, “A Review on Surface Modification of Plant Fibers for Enhancing Properties of Biocomposites,” *ChemistrySelect*, vol. 9, no. 21, p. e202400650, Jun. 2024, doi: 10.1002/slct.202400650.

[6] K. Li, R. Qiu, and W. Liu, “Improvement of Interfacial Adhesion in Natural Plant Fiber-reinforced Unsaturated Polyester Composites: A Critical Review,” *Rev. Adhes. Adhes.*, vol. 3, no. 1, pp. 98–120, Mar. 2015, doi: 10.7569/RAA.2015.097301.

[7] A. A. Mohammed, D. Bachtiar, M. R. M. Rejab, S. F. Hasany, and J. P. Siregar, “Influence of Different Sugar Palm Fiber Content on the Tensile, Flexural, Impact, and Physicochemical Properties of Eco-Friendly Thermoplastic Polyurethane,” *Theor. Found. Chem. Eng.*, vol. 53, no. 3, pp. 454–462, May 2019, doi: 10.1134/S0040579519030072.

[8] D. Ginting and R. N. Fitri, “Efek Sintesis Silane Coupling Agent Pada Sifat Fisis dan Mekanis Komposit Serbuk Kenaf,” *J. Fis. Fis. Sains Dan Apl.*, vol. 6, no. 2, pp. 113–117, Oct. 2021, doi: 10.35508/fisa.v6i2.6841.

[9] S. Hastuti, H. S. Budiono, D. I. Ivadiyanto, and M. N. Nahar, “Peningkatan Sifat Mekanik Komposit Serat Alam Limbah Sabut Kelapa (Cocofiber) yang Biodegradable,” *Reka Buana J. Ilm. Tek. Sipil Dan Tek. Kim.*, vol. 6, no. 1, pp. 30–37, Mar. 2021, doi: 10.33366/rekabuana.v6i1.2257.

[10] S. K. Ramamoorthy, M. Skrifvars, and M. Rissanen, “Effect of alkali and silane surface treatments on regenerated cellulose fibre type (Lyocell) intended for composites,” *Cellulose*, vol. 22, no. 1, pp. 637–654, Feb. 2015, doi: 10.1007/s10570-014-0526-6.

[11] O. Fadele, I. N. A. Oguocha, A. G. Odeshi, M. Soleimani, and L. G. Tabil, “Effect of chemical treatments on properties of raffia palm (Raphia farinifera) fibers,” *Cellulose*, vol. 26, no. 18, pp. 9463–9482, Dec. 2019, doi: 10.1007/s10570-019-02764-8.

[12] Md. S. Islam, Z. A. Talib, A. K. Azad, and A. Kaiser, “Chemical Modifications and Properties of Coir Fibers Biocomposites,” in *Agricultural Biomass Based Potential Materials*, K. R. Hakeem, M. Jawaid, and O. Y. Alothman, Eds., Cham: Springer International Publishing, 2015, pp. 491–505, doi: 10.1007/978-3-319-13847-3_23.

[13] F. Pakaya *et al.*, “Arenga pinnata Merr. Reinforced Polyester Biocomposite as a Candidate Material for Fishing Vessel Hull: Mechanical Properties Analysis,” *Marit. Park J. Marit. Technol. Soc.*, May 2025, doi: 10.62012/mp.vi.43650.

[14] M. N. Norizan, K. Abdan, M. S. Salit, and R. Mohamed, “Physical, Mechanical and Thermal Properties of Sugar Palm

Yarn Fibre Loading on Reinforced Unsaturated Polyester Composites," *J. Phys. Sci.*, vol. 28, no. 3, Nov. 2017, doi: 10.21315/jps2017.28.3.8.
[15] R. M. Shahroze *et al.*, "Sugar palm fiber/polyester nanocomposites: Influence of adding nanoclay fillers on thermal, dynamic mechanical, and physical properties," *J. Vinyl Addit. Technol.*, vol. 26, no. 3, pp. 236–243, Aug. 2020, doi: 10.1002/vnl.21736.
[16] M. N. Norizan, K. Abdan, M. S. Salit, and R. Mohamed, "The Effect of Alkaline Treatment on the Mechanical Properties of Treated Sugar Palm Yarn Fibre Reinforced Unsaturated Polyester Composites Reinforced with Different Fibre loadings of Sugar Palm Fibre," *Sains Malays.*, vol. 47, no. 4, pp. 699–705, Apr. 2018, doi: 10.17576/jsm-2018-4704-07.
[17] A. Atiqah, M. Jawaid, S. M. Sapuan, and M. R. Ishak, "Effect of Surface Treatment on the Mechanical Properties of Sugar Palm/Glass Fiber-reinforced Thermoplastic Polyurethane Hybrid Composites," *BioResources*, vol. 13, no. 1, pp. 1174–1188, Dec. 2017, doi: 10.15376/biores.13.1.1174-1188.
[18] A. Atiqah, M. Jawaid, S. M. Sapuan, M. R. Ishak, M. N. M. Ansari, and R. A. Ilyas, "Physical and thermal properties of treated sugar palm/glass fibre reinforced thermoplastic polyurethane hybrid composites," *J. Mater. Res. Technol.*, vol. 8, no. 5, pp. 3726–3732, Sep. 2019, doi: 10.1016/j.jmrt.2019.06.032.
[19] I. Mukhtar, Z. Leman, E. S. Zainudin, and M. R. Ishak, "Hybrid and Nonhybrid Laminate Composites of Sugar Palm and Glass Fibre-Reinforced Polypropylene: Effect of Alkali and Sodium Bicarbonate Treatments," *Int. J. Polym. Sci.*, vol. 2019, pp. 1–12, Apr. 2019, doi: 10.1155/2019/1230592.
[20] N. M. Nurazzi, A. Khalina, S. M. Sapuan, and R. A. Ilyas, "Mechanical properties of sugar palm yarn/woven glass fiber reinforced unsaturated polyester composites: effect of fiber loadings and alkaline treatment," *Polimery*, vol. 64, pp. 665–675, 2019, doi: 10.14314/polimery.2019.10.3.
[21] N. M. Nurazzi, "Effect of fiber orientation and fiber loading on the mechanical and thermal properties of sugar palm yarn fiber reinforced unsaturated polyester resin composites," *Polimery*, vol. 65, no. 2, pp. 115–124, 2020, doi: 10.14314/polimery.2020.2.5.
[22] N. M. Nurazzi, A. Khalina, S. M. Sapuan, R. A. Ilyas, S. A. Rafiqah, and Z. M. Hanafee, "Thermal properties of treated sugar palm yarn/glass fiber reinforced unsaturated polyester hybrid composites," *J. Mater. Res. Technol.*, vol. 9, no. 2, pp. 1606–1618, Mar. 2020, doi: 10.1016/j.jmrt.2019.11.086.
[23] J. H. Aurer and A. Kasper, *Unsaturated Polyester Resins*. in 1. BÜFA Reaktionsharze GmbH & Co. KG and DSM Composite Resins AG, 2003.
[24] F. Fatkhurrohman, I. Ismail, and F. Yudhanto, "Analisis Kekuatan Bending Komposit Lamina Serat Ijuk Anyam dan Serat Ijuk Acak bermatriks Polyester," *Quantum Tek. J. Tek. Mesin Terap.*, vol. 4, no. 1, pp. 55–61, Dec. 2022, doi: 10.18196/jqt.v4i1.16593.
[25] A. M. N. Maisara, R. A. Ilyas, S. M. Sapuan, M. R. M. Huzaifah, N. M. Nurazzi, and S. O. A. SaifulAzry, "Effect of Fibre Length and Sea Water Treatment on Mechanical Properties of Sugar Palm Fibre Reinforced Unsaturated Polyester Composites," *Int. J. Recent Technol. Eng.*, vol. 8, no. 2S4, pp. 510–514, Aug. 2019, doi: 10.35940/ijrte.B1100.0782S419.
[26] S. Sudarisman, S. Hamdan, H. Sosiati, and K. Krisdiyanto, "The effect of hybrid ratio on the flexural properties of Arenga Pinnata fiber/E-glass fiber/polyester hybrid composites," *J. Appl. Res. Technol.*, vol.22, n.1, pp.59-66, 2024, doi: 10.22201/icat.24486736e.2024.22.1.2176
[27] M. R. M. Asyraf *et al.*, "Sugar Palm Fibre-Reinforced Polymer Composites: Influence of Chemical Treatments on Its Mechanical Properties," *Materials*, vol. 15, no. 11, p. 3852, May 2022, doi: 10.3390/ma15113852.
[28] F. S. M. Radzi *et al.*, "Effect of reinforcement of Alkaline-treated sugar palm/bamboo/kenaf and fibreglass/ Kevlar with polyester hybrid biocomposites: mechanical, morphological, and water absorption properties," *J. Mater. Res. Technol.*, vol. 24, 2023, doi: 10.1016/j.jmrt.2023.04.055.
[29] M. R. M. Huzaifah, S. M. Sapuan, Z. Leman, and M. R. Ishak, "Effect of Fibre Loading on the Physical, Mechanical and Thermal Properties of Sugar Palm Fibre Reinforced Vinyl Ester Composites," *Fibers Polym.*, vol. 20, no. 5, pp. 1077–1084, May 2019, doi: 10.1007/s12221-019-1040-0.
[30] R. Srinivasan, S. P. M, R. G, and M. A. Murugan, "Influence of alkali–silane treatment on pistachio shell lignin and sunn hemp fiber-reinforced epoxy bio-composites: A characterization approach," *J. Therm. Anal. Calorim.*, vol. 150, no. 26, pp. 21479–21489, Dec. 2025, doi: 10.1007/s10973-025-15045-3.